Title	Computational study on ice growth inhibition of Antarctic bacterium antifreeze protein using coarse grained simulation
Author(s)	Nguyen, Hung; Le, Ly; Ho, Tu Bao
Citation	Journal of Chemical Physics, 140(22): 225101-1-225101-8
Issue Date	2014-06-11
Type	Journal Article
Text version	publisher
URL	http://hdl.handle.net/10119/12349
Rights	Copyright 2014 American Institute of Physics. This article may be downloaded for personal use only. Any other use requires prior permission of the author and the American Institute of Physics. The following article appeared in Hung Nguyen, Ly Le, and Tu Bao Ho, Journal of Chemical Physics, 140(22), 225101 (2014) and may be found at http://dx.doi.org/10.1063/1.4881895
Description	

Computational study on ice growth inhibition of Antarctic bacterium antifreeze protein using coarse grained simulation

Hung Nguyen, Ly Le, and Tu Bao Ho

Articles you may be interested in

A coarse grain model for protein-surface interactions
J. Chem. Phys. **139**, 095102 (2013); 10.1063/1.4819131

Influence of mobile DNA-protein-DNA bridges on DNA configurations: Coarse-grained Monte-Carlo simulations
J. Chem. Phys. **135**, 125104 (2011); 10.1063/1.3636383

Monte Carlo study of the molecular mechanisms of surface-layer protein self-assembly
J. Chem. Phys. **134**, 125103 (2011); 10.1063/1.3565457

Residue energy and mobility in sequence to global structure and dynamics of a HIV-1 protease (1DIFA) by a coarse-grained Monte Carlo simulation
J. Chem. Phys. **130**, 044906 (2009); 10.1063/1.3050106

The role of sidechain packing and native contact interactions in folding: Discontinuous molecular dynamics folding simulations of an all-atom G model of fragment B of Staphylococcal protein A
J. Chem. Phys. **117**, 8983 (2002); 10.1063/1.1514574

Computational study on ice growth inhibition of Antarctic bacterium antifreeze protein using coarse grained simulation

Hung Nguyen,[1] Ly Le,[1,2,a)] and Tu Bao Ho[3]

[1]*Life Science Laboratory of the Institute for Computational Science and Technology at Ho Chi Minh City, Vietnam*

[2]*School of Biotechnology of Ho Chi Minh International University, Vietnam National University, Ho Chi Minh City, Vietnam*

[3]*School of Knowledge Science of Japan Advanced Institute of Science and Technology, Nomi, Ishikawa, Japan*

Antarctic bacterium antifreeze proteins (AFPs) protect and support the survival of cold-adapted organisms by binding and inhibiting the growth of ice crystals. The mechanism of the anti-freezing process in a water environment at low temperature of Antarctic bacterium AFPs remains unclear. In this research, we study the effects of Antarctic bacterium AFPs by coarse grained simulations solution at a temperature range from 262 to 273 K. The results indicated that Antarctic bacterium AFPs were fully active in temperatures greater than 265 K. Additionally, the specific temperature ranges at which the water molecules become completely frozen, partially frozen, and not frozen were identified. © 2014 AIP Publishing LLC. [http://dx.doi.org/10.1063/1.4881895]

I. INTRODUCTION

Many organisms that live in cold climates produce several specific types of proteins including antifreeze proteins (AFPs) and antifreeze glycoprotein (AFGPs)[1] in order to inhibit growth of ice within their body fluids and support their survival during winter condition.[2,3] Especially, the AFPs found in a variety of organisms such as fishes,[4–6] insects,[7–9] plants,[10,11] and bacteria[12,13] have the ability to prevent the formation and recrystallization of ice at extremely low temperatures[2] by adsorbing on the ice surface. This mechanism was considered as recrystallization inhibition.[14,15] Therefore, liquid water does not completely form ice when it contains AFPs, even at significantly lower temperatures than the melting point of ice.[2] In cold environments, some bacteria and plants that cannot avoid freezing use AFPs to lessen the destructive effects of ice recrystallization. These AFPs have weak freezing point depression activity in order to avoid the uncontrolled growth of ice. The mechanism by which AFPs irreversibly bind to ice has not been fully understood.[14]

The binding site of AFPs was relatively hydrophobic and also contained many potential hydrogen bond donors/acceptors. The extent to which hydrogen bonds and the hydrophobic effects contributed to ice binding has been debated for over last 30 years.[16,17] These problems had been elucidated by the ice binding mechanisms and the first crystal structure of Antarctic bacterium AFPs. The largest AFPs demonstrated that folds or Ca^{2+}-bound parallel beta-helices with an extensive array of ice-like surface waters were anchored via hydrogen bonds directly to the polypeptide backbone and adjacent side chains.[17]

The AFPs produce the difference between the freezing and the melting temperature, which was identified as thermal hysteresis (TH) which has been used as a characteristic to measure AFPs activity.[2,14,18,19] The presence of TH activity of bacteria was first demonstrated by Duman and Olsen.[20] AFPs can reduce the freezing point of aqueous fluids below the melting point of ice. Subsequently, a number of cold-adapted bacteria have been found to possess AFPs with a proportional fraction to their body size including Antarctic isolates. As a result, the roles of bacterial AFPs in cold environment have been indicated.[16] Some TH values were found to be associated with AFPs isolated from insects (3–6 °C), fishes (0.7–1.5 °C), plants (0.2–0.5 °C), and bacteria (less than 0.1 °C).[15] Therefore, it was certain that AFPs in animals work by the mechanism of freeze avoidance, and mechanism of freeze tolerance was also the strategy used by the AFPs occurring in plants and bacteria. The Antarctic bacterium AFPs could additionally perform the mechanism of freeze avoidance.[15]

In this research, we focused on the different effects of Antarctic bacterium AFPs in NaCl environment at a concentration of 0.6 mol/l at low temperatures. In comparison and review the inhibition ability in the salt liquid freezing process of Antarctic bacterium AFPs, the freezing process of salt solution surrounding proteins and other related values of water-ice structures were observed by coarse grained simulations.

II. MATERIALS AND METHODS

A. Preparation the protein structures for MD simulations

The 3D structure of Antarctic bacterium AFPs was taken from Protein Data Bank (PDB) with PDB entry 3P4G.[17] The Visual Molecular Dynamics (VMD) software[21] was employed to create the monomer structure of full-atom structure (Fig. 1(a)). And then, MARTINIZE version 2.2 was applied to convert full-atom Antarctic bacterium AFPs structure

a)E-mail: ly.le@hcmiu.edu.vn
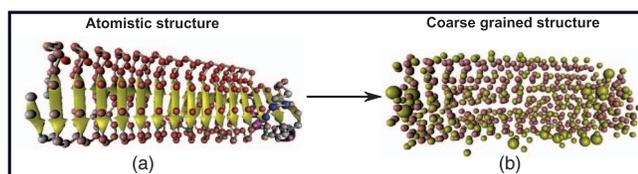
FIG. 1. Image illustrates the atomistic structure (the beads are CA^{2+} ions) (Fig. 1(a)) and coarse grained structure (Fig. 1(b)) of Antarctic bacterium AFPs.

existing in PDB format into coarse grained beads[22] (Fig. 1(b)). In coarse grained model, each amino acid was modeled by one or two beads according to their specific sizes, which can be classified into two broad categories: backbone beads and side chain beads. The side chain and backbone beads can be denoted as SC_i (i = ARG, GLN, GLU, HIS, ILE, LYS, MET, PHE, TRP, TYR) and BB_i (i = ALA, ASN, ASP, CYS, GLY, LEU, PRO, SER, THR, VAL), respectively.

B. Simulation methods

All MD simulations were performed using GROMACS 4.5 package[23] with MARTINI force field for coarse grained model. The periodic boundary conditions were used throughout the simulation process; the electrostatic potential was shifted from 0.0 nm to 1.2 nm and the Lennard Jones (LJ) potential was shifted from 0.9 nm to 1.2 nm on all three axes (x, y, and z).[24] The complexes of Antarctic bacterium AFPs were positioned inside a cubic box at a distance of 1.2 nm from the solute and the box wall; the water model was used specifically in coarse grained model (here was MARTINI force field).

The minimization was converged when the maximum force became smaller than 0.01 kJ/mol/nm; the steepest descent simulation for minimization was performed over 5000

steps. The equilibration was performed coupling with temperature and pressure. Constant temperature 303 K was enforced using Berendsen algorithm[25] under 1 ns for constant volume and temperature (NVT) simulation with a damping coefficient of 0.1 ps; Parrinello-Rahman pressure[26] was coupled in 1.5 ns constant pressure and temperature (NPT) run at 1 bar constant pressure with the damping coefficient of 0.1 ps. The structures were generated as the configurations for our MD simulation with 12 temperatures including 262 K, 263 K, 264 K, 265 K, 266 K, 267 K, 268 K, 269 K, 270 K, 271 K, 272 K, and 273 K. In addition, we also generated complex structure at 278 K for comparison. The final MD simulation allowed us to integrate the equations of motion with a time step of 1 fs and our simulation run for totally 100 ns in the leap-frog algorithm.[27]

III. RESULTS AND DISCUSSION

The stability of simulation complex was explored by root mean square deviation (RMSD), which related to initial complex structures. RMSD values of Antarctic bacterium AFPs (Figs. 2(a) and 2(b)) presented large variations in magnitude and interactions between Antarctic bacterium AFPs residues and water molecules. It is reasonable that available Ca^{2+} ions in the original structure of the Antarctic bacterium AFPs play a key role in contributing to inhibit their water freezing process at low temperatures. The RMSD results for 12 temperatures were divided into two separate states: from 262 K to 267 K (Fig. 2(a)), and 268 K and over (Fig. 2(b)). In the former, RMSD fluctuated slightly in the first 20 ns and then remained stable at under 0.7 nm. However, the latter saw the significant fluctuations in RMSD, which indicated strong interactions between proteins and other molecules in the simulation systems (here, other molecules were included: water molecules, Na$^+$ and Cl$^-$ ions). Especially, the RMSD of Antarctic bacterium AFPs at 270 K was remarkably
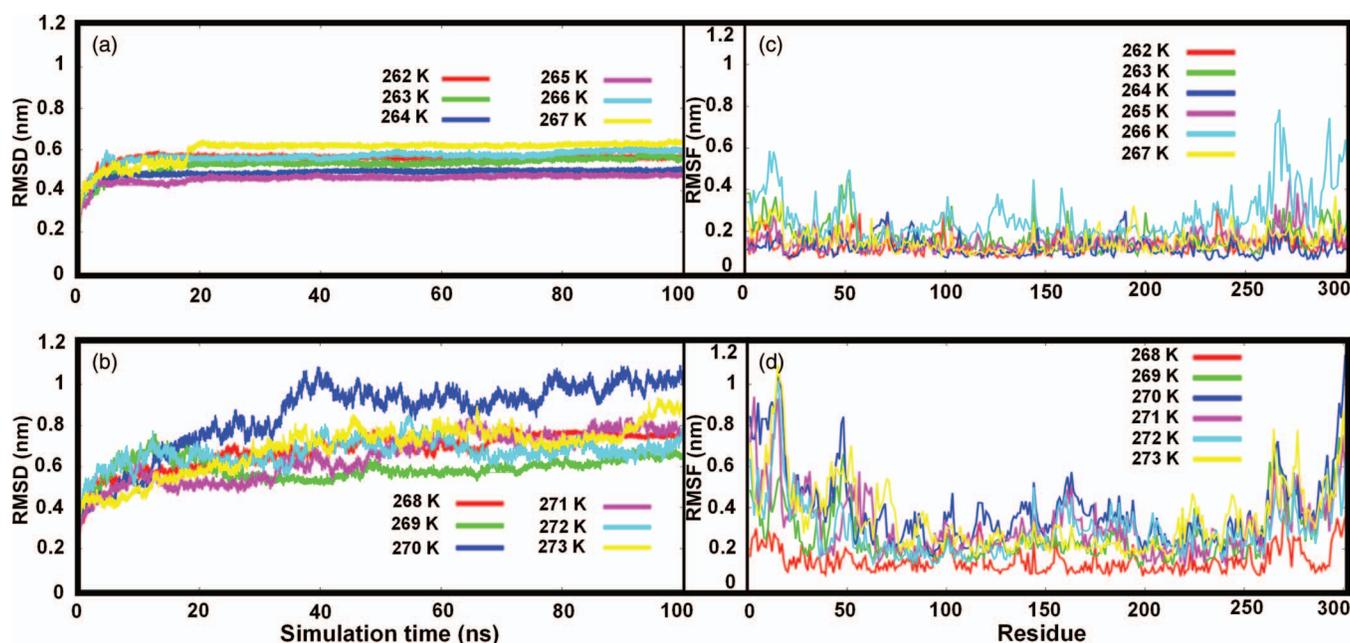
FIG. 2. Root mean square deviation (RMSD) (Figs. 2(a) and 2(b)) and root mean square fluctuation (RMSF) (Figs. 2(c) and 2(d)) values of Antarctic bacterium AFPs.
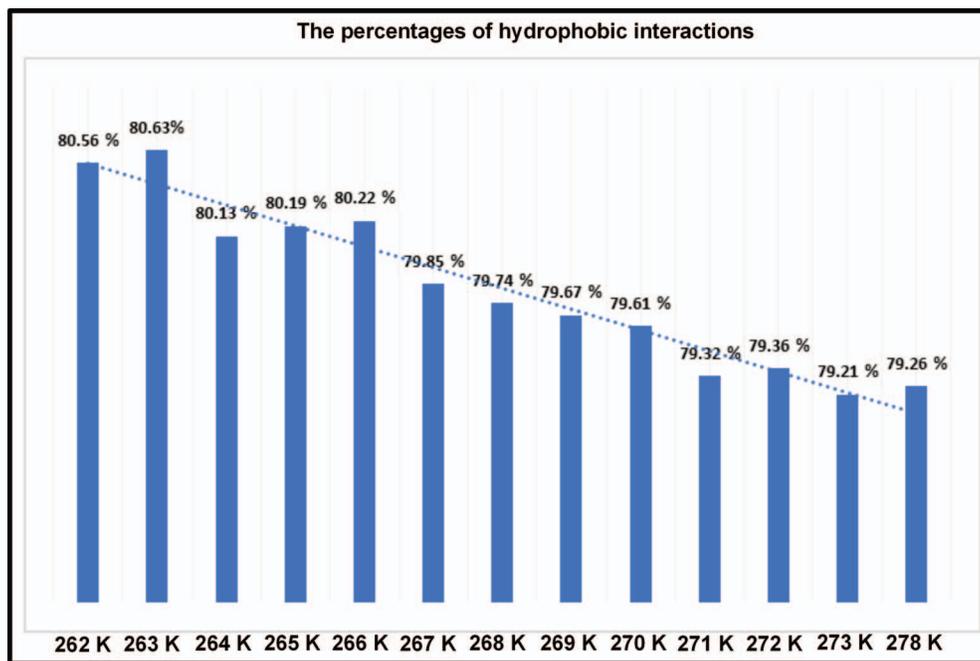
FIG. 3. The percentages of hydrophobic interactions of Antarctic bacterium AFPs were calculated from 262 K to 273 K and 278 K.

highest throughout the simulation systems with the peak value of 1.0226 nm.

Besides, the root mean square fluctuation (RMSF) of Antarctic bacterium AFPs, showed in Figs. 2(c) and 2(d), presented the characteristic variation of each residue in the whole simulation process. Similarly to the RMSD's results, the RMSF values presented changes along the simulation temperature range of Antarctic bacterium AFPs. The RMSF values of Antarctic bacterium AFP residues (Fig. 2(c)) were fluctuated lower than 0.8 nm. From 269 K to 273 K, the RMSF started fluctuating strongly, especially at the first 65 residues and the last 43 residues during complex simulation (Fig. 2(d)). The RMSF value of Antarctic bacterium AFPs at 270 K contained the numbered residue 301 reached the level of 1.1403 nm, which was also the largest value in the whole results. From these results, it can be defined that all hydrophobic residues in AFPs could interact strongly with water molecules, Na^+ and Cl^- ions; thereby inhibit the freezing process of water molecules at low temperatures. These results were further investigated more details in Sec. IV.

In Fig. 3, the hydrophobic residues would be bounded to ice crystals and hydrophilic residues were exposed to liquid water. The interactions of hydrophobic residues with ice would produce entropy while those hydrophilic residues exposed to liquid water surrounding formed vaguely hexagonal shapes (cage-like structures). The exposure process of hydrophilic residues to liquid water would produce enthalpy and possibly lead to the rearrangement of liquid water molecules to form hydrogen bonds with hydrophilic residues. From entropy and enthalpy achievements, this finding has shed some light on the reasons why ice binding regions of Antarctic bacterium AFPs are various at different temperatures.

The radial distribution function was used when water structures were studied. The aqueous solution was frozen at extremely low temperatures and formed the ice structure net-

work under the vaguely hexagonal shape.[28,29] The ice structure network would be gradually enhanced with the simulation time, thereby probably expand the influenced region of ice crystals in the whole simulation space. The activity of liquid water will be reduced and completely inhibited in order to form the crystal structure (crystallize or recrystallize process). The thermodynamic process would be subsided and most
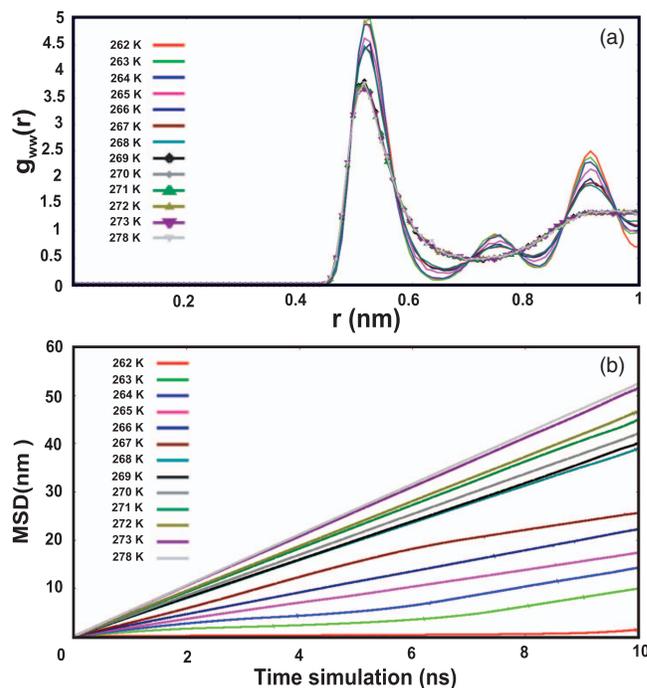
FIG. 4. Water-water radial distribution function ($g_{ww}(r)$) is shown in Fig. 4(a) (the results described were the last frame of 100 ns simulation) and Fig. 4(b) illustrated mean square displacement (MSD) values as a function of time in 10 ns simulation time.
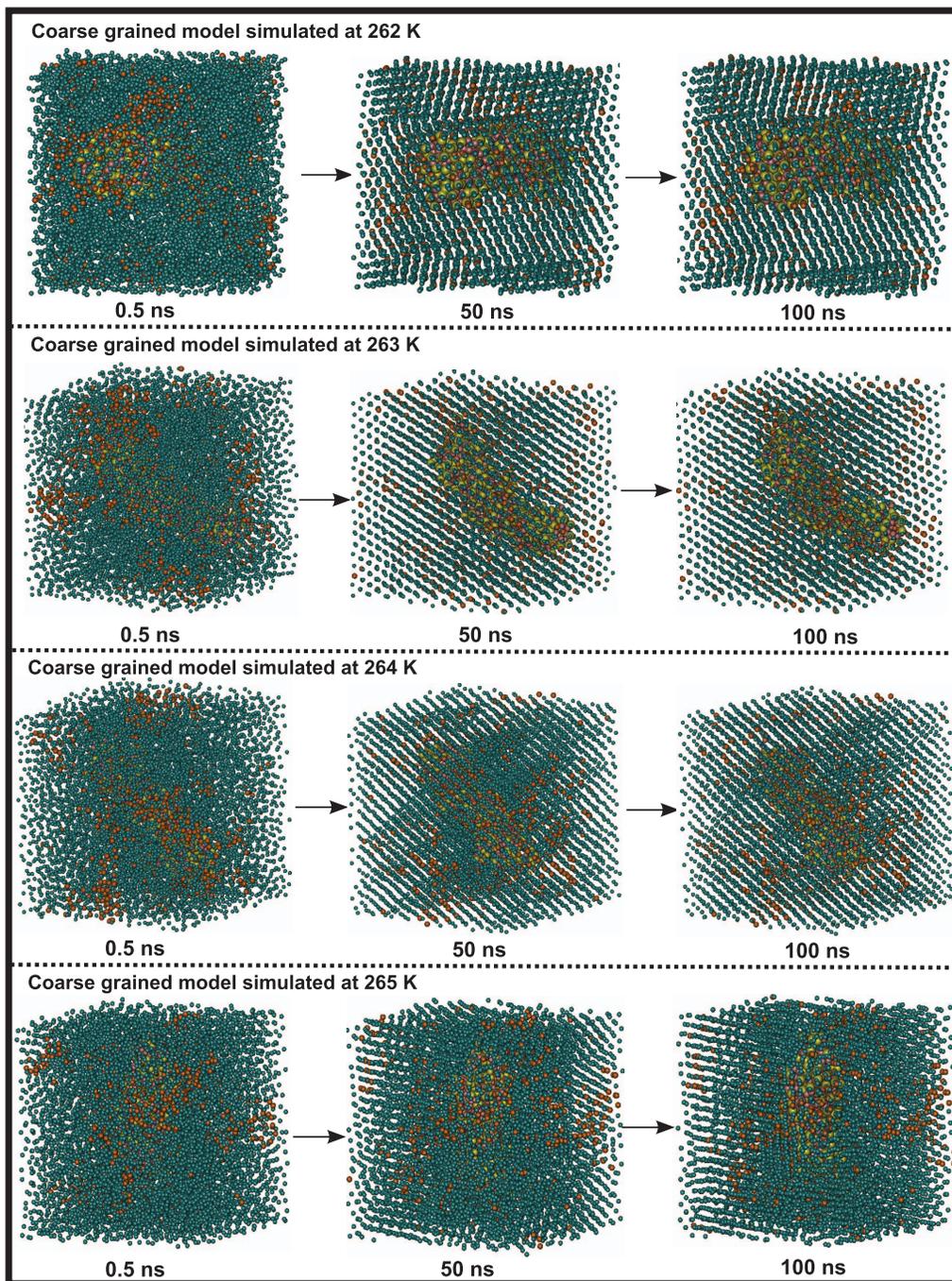
FIG. 5. The snapshots showed the freezing process of Antarctic bacterium AFPs in NaCl environment from 262 K to 265 K, respectively. It was shown by VMD software.

activities of the creatures living in ice environment will be completely paralyzed. In general, the $g_{ww}(r)$ value has proved that water molecules have ability to form the ice crystal structures or ice-water structures, or maintain liquid solution. The $g_{ww}(r)$ of water-water beads surrounded Antarctic bacterium AFPs for coarse grained model (Fig. 4(a)) was distinguished among different temperatures from 262 K to 273 K. Here, it could be divided into three stages based on $g_{ww}(r)$ values: First, from 262 K to 264 K, the $g_{ww}(r)$ fluctuated around the r distance of 2.5 nm, and water molecules existed in ice array formation completely (100% ice crystal structures). The height of three peaks from 262 K to 264 K decreased when

the temperatures increased, which was inversely proportional. Second, from 265 K to 268 K, the $g_{ww}(r)$ values reached from 1.55 nm to 2.45 nm. From this it could be inferred that water molecules around Antarctic bacterium AFPs became partially frozen and the ratio of ice existence in the complex mainly depended on the simulation temperatures. For instance, water molecules at 265 K formed ice crystals more than liquid water and when the temperature increased to 268 K, the ice crystals were formed less than liquid water. Finally, from 269 K to 273 K, the $g_{ww}(r)$ values remained stable at 1.375 nm, water molecules were entirely in a liquid state. In addition, we also show the $g_{ww}(r)$ of 278 K to compare with 12 temperatures
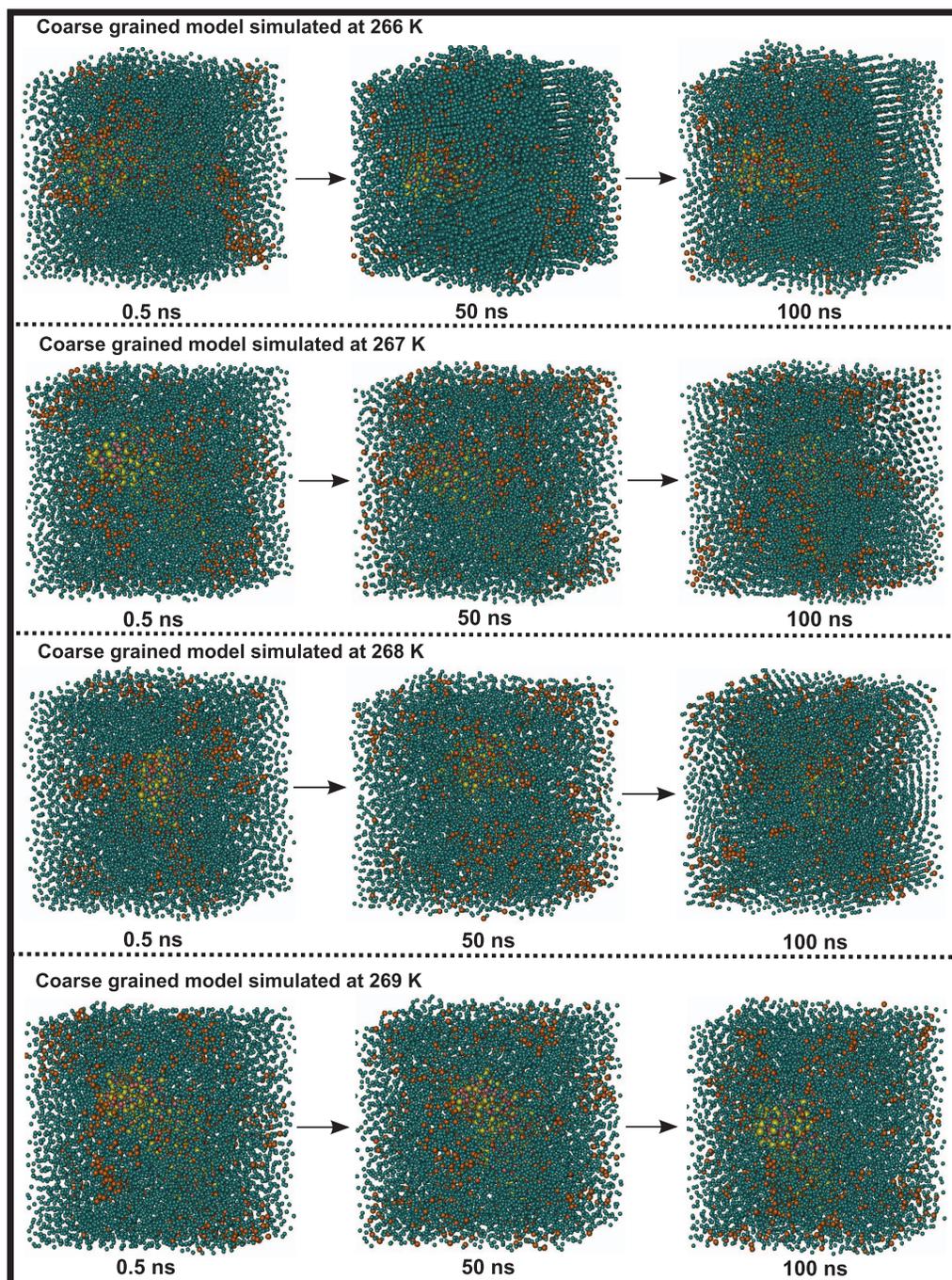
FIG. 6. The snapshots showed the freezing process of Antarctic bacterium AFPs in NaCl environment from 266 K to 269 K, respectively. It was shown by VMD software.

above, and this value is overlapped with the $g_{ww}(r)$ of temperatures from 269 K to 273 K. These findings will be mentioned in detail in some snapshots below (Figs. 5 and 6). Hence it could be confirmed that Antarctic bacterium AFPs were only activated by the ability of inhibiting the ice growth at the temperatures greater than 265 K, which is in agreement with the prior experimental results. Simultaneously, mean square displacement (MSD) results of water in Fig. 4(b) also indicated that the restraints restricted the diffusion adequately. The MSD values were calculated for 10 ns of stable simulation. These images became interferences when time increased. We see that the MSD values increased when the tem-

peratures increased; the smallest result was at 262 K and the largest at 278 K.

The simulations provide a clue as to how the freezing transition happens at lower temperature for Antarctic bacterium AFPs. Figs. 5 and 6 show snapshots of Antarctic bacterium AFPs and surrounding water molecules during the growth of ice and Antarctic bacterium AFPs partially surrounded by the growth of ice during the simulation. Here, each figure showed complex structures at 0.5 ns, 50 ns, and 100 ns simulation time at four different temperatures. In Fig. 5, we present the snapshots of Antarctic bacterium AFPs, water molecules, Na$^+$ and Cl$^-$ ions in simulation complexes
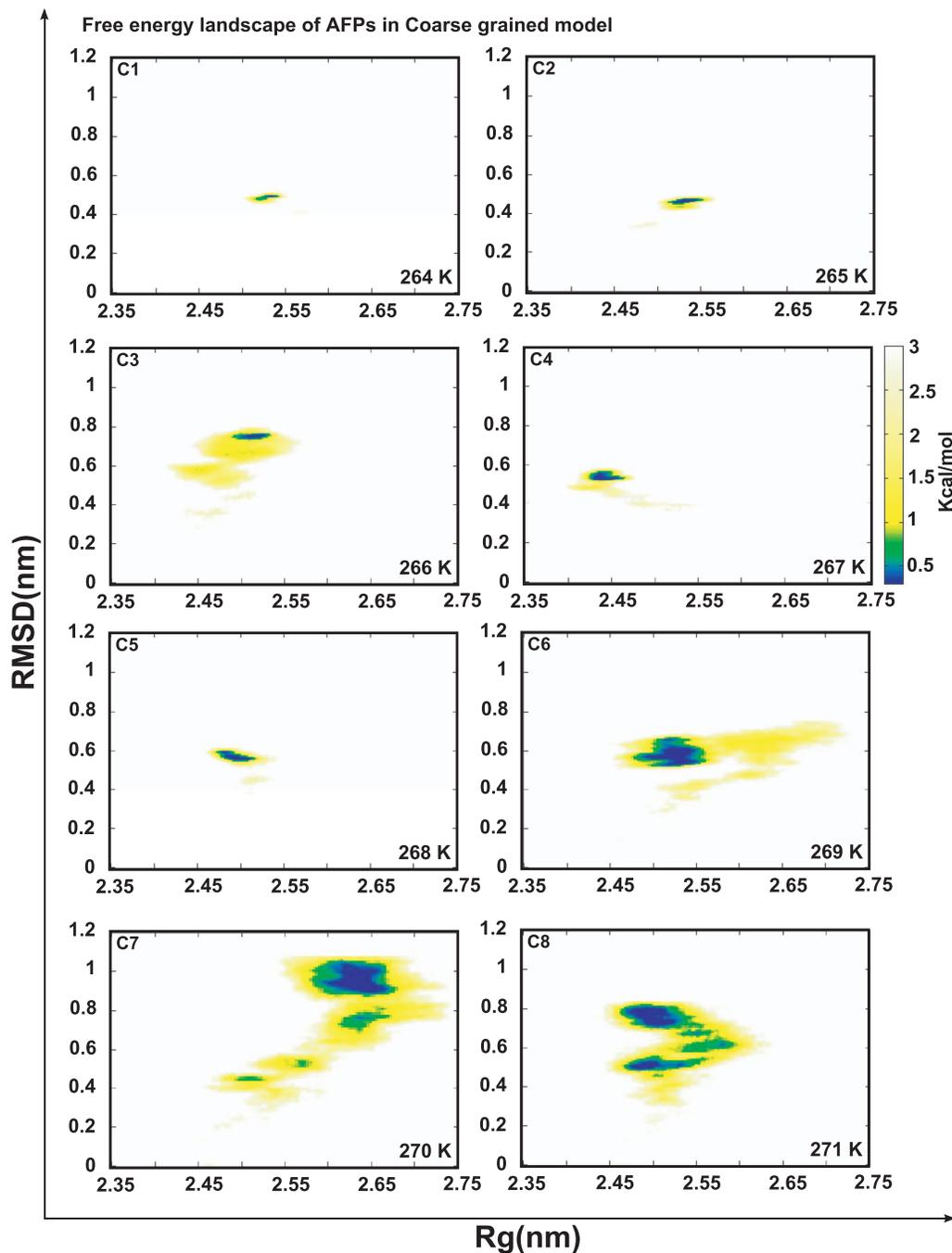
FIG. 7. Free energy landscape of Antarctic bacterium AFPs from 264 K to 271 K. RMSD stands for root mean square deviation of protein and Rg represents the radius of gyration of protein.

at 262 K, 263 K, 264 K, and 265 K, respectively. It can be seen that from 262 K to 264 K, the water molecules were not frozen at 0.5 ns, but were completely frozen after 50 ns simulation. There was a difference between the crystal structures of ice forming at 262 K and those at 263 K and 264 K. Whereas the growth of ice crystals at 262 K did not follow certain directions, and be interspersed between segments; at 263 K and 264 K, the ice crystals were formed in a certain direction, which were stacked between the ice arrays. Actually, the ice formation only occurs randomly, so it is not a special problem. With the complex at 265 K, the ice crystals in the complex were much more than liquid water components,

only a small amount of liquid water existed around Antarctic bacterium AFPs.

Fig. 6 showed the snapshots of complexes at temperatures from 266 K to 269 K. From 266 K to 268 K, the water molecules transformed partially into ice crystal structures around Antarctic bacterium AFPs, the ice formations in these temperatures gradually reduced when the temperatures increased. The ice crystals in the complex were less than liquid water components. Apparently, the ratio of ice to liquid water in these three temperatures was insignificantly small. Otherwise, the water molecules around the Antarctic bacterium AFPs were completely in the form of liquid water when

temperature was equal or greater than 269 K. These snapshots provide useful background to identify different temperature ranges that Antarctic bacterium AFPs can be activated in NaCl environment.

In this work, the free energy landscape was employed to determine the most stable structure of the complex system corresponding to local energy minimum point. The typical structures from the simulation were also chosen from free energy landscape via choosing the minimum regions of free energy landscape values. Hence, the ice binding site of Antarctic bacterium AFPs could be determined via local energy minimum regions on free energy landscape. Fig. 7 shows the free energy landscape for the Antarctic bacterium AFPs structure at different temperatures from 264 K to 271 K. These values of the Antarctic bacterium AFPs structure are the most stable and repeated abundantly with minimum free energy values. There were significant changes of magnitude in minimum free energy regions, which was extended along when the temperatures increased. The residues of protein fluctuated strongly when the bound of ice crystal structure and the complex was not frozen at low temperatures, leading to the expansion of free energy minimum regions. At those temperatures, Antarctic bacterium AFPs have enough conditions to activate the freezing process inhibition of liquid water (normally at those temperatures water is frozen). Meanwhile, side chains in Antarctic bacterium AFPs that act strongly will form much more configurations having tendency to stabilize. That is the reason why, with the complexes at high temperatures, the area of local minimum energy region is much larger. The number of structures accepted as stable structures was also identified easily. In detail, free energy landscapes for temperatures from 264 K to 268 K have smaller local minimum energy regions compared with those for temperatures equal and greater than 269 K.

IV. CONCLUSIONS

In conclusion, the results from our simulations have shed some light into the exact mechanism of Antarctic bacterium AFPs in NaCl environment among various temperatures ranging from 262 K to 273 K. This study pointed out that Antarctic bacterium has the capability to inhibit the freezing process of water at low temperatures. In addition, we also identified specific temperature ranges at which water molecules become completely frozen (from 262 K to 264 K), partially frozen (from 265 K to 268 K), and not frozen (the temperatures are greater than 268 K). As a result, we can identify action temperature ranges at which Antarctic bacterium AFPs can exist at low temperature environment.

In general, freezing of water is a slow process in comparison with time scale in simulation. The coarse grained models allow us to overcome this limitation and to capture the role of anti-freezing protein with affordable computing expense. However, with coarse grained models, we lost some detailed information, specifically, the effect of protonated amino acids near Ca^{2+} on ice formation. Further studies at lower salt concentration with atomistic MD simulation are strongly recommended.

[1]Y. Yeh and R. E. Feeney, "Antifreeze proteins: Structures and mechanisms of function," Chem. Rev. **96**, 601–618 (1996).

[2]H. Nada and Y. Furukawa, "Antifreeze proteins: Computer simulation studies on the mechanism of ice growth inhibition," Polym. J. **44**, 690–698 (2012).

[3]E. Kristiansen, E. Wilkens, B. Vincents, D. Friis, A. B. Lorentzen, H. Jenssen, A. Lobner-Olesen, and H. Ramlov, "Hyperactive antifreeze proteins from longhorn beetles: Some structural insights," Insects Physiol. **58**, 1502–1510 (2012).

[4]A. L. DeVries, S. K. Komatsu, and R. E. Feeney, "Chemical and physical properties of freezing point depressing glycoproteins from Antarctic fishes," Biol. Chem. **245**, 2901–2908 (1970).

[5]P. L. Davies, C. L. Hew, and G. L. Fletcher, "Fish antifreeze proteins: Physiology and evolutionary biology," Can. J. Zool. **66**, 2611–2617 (1980).

[6]C. B. Marshall, G. L. Fletcher, and P. L. Davies, "Hyperactive antifreeze protein in a fish," Nature (London) **429**, 153 (2004).

[7]C. L. Hew, M. H. Kao, Y.-P. So, and K.-P Lim, "Presence of cystine-containing antifreeze proteins in the spruce budworm, *Choristoneura fumiferana*," Can. J. Zool. **61**, 2324–2328 (1983).

[8]R. Schneppenheim and H. Theede, "Isolation and characterization of freezing-point depressing peptides from larvae of *Tenebrio molitor*," Comp. Biochem. Physiol., Part B: Biochem. Mol. Biol. **67**, 561–568 (1980).

[9]J. G. Duman, V. Bennett, T. Sformo, R. Hochstrasser, and B. M. Barnes, "Anti-freeze proteins in Alaskan insects and spiders," Insects Physiol. **50**, 259–266 (2004).

[10]O. Atıcı and B. Nalbantoglu, "Antifreeze proteins in higher plants," Phytochemistry **64**, 1187–1196 (2003).

[11]M. Griffith and M. W. F. Yaish, "Antifreeze proteins in overwintering plants: A tale of two activities," Trends Plant Sci. **9**, 399–405 (2004).

[12]K. Meister, S. Ebbinghaus, Y. Xu, G. D. John, A. DeVries, M. Gruebele, M. L. David, and M. Havenith, "Long-range protein-water dynamics in hyperactive insect antifreeze proteins," Proc. Natl. Acad. Sci. U.S.A. **110**, 1617–1622 (2012).

[13]C. Yang and A. S. Kim, "The mechanism of the type III antifreeze protein action: A computational study," Biophys. Chem. **109**, 137–148 (2004).

[14]A. G. Jack, L. D. Peter, and L.-P. Johanna, "A hyperactive, Ca^{2+} - dependent antifreeze protein in an Antarctic bacterium," FEMS Microbiol. Lett. **245**, 67–72 (2005).

[15]M. K. Chattopadhyay, "Antifreeze proteins of bacteria," Resonance **12**, 25–30 (2007).

[16]P. L. Davies, J. Baardsnes, M. J. Kuiper, and V. K. Walker, "Structure and function of antifreeze proteins," Philos. Trans. R. Soc. Lond. B **357**, 927–935 (2002).

[17]P. G. Christopher, L. C. Robert, and L. D. Peter, "Anchored clathrate waters bind antifreeze proteins to ice," Proc. Natl. Acad. Sci. U.S.A. **108**, 7363–7367 (2011).

[18]P. G. Christopher, A. G. Jack, P. H. Christopher, L. C. Robert, L.-P. Johanna, and L. D. Peter, "A Ca^{2+}-dependent bacterial antifreeze protein domain has a novel β-helical ice-binding fold," Proc. Natl. Acad. Sci. U.S.A. **411**, 171–180 (2008).

[19]H. Kondo, Y. Hanada, H. Sugimoto, T. Hoshino, P. G. Christopher, and L. D. Peter, "Ice-binding site of snow mold fungus antifreeze protein deviates from structural regularity and high conservation," Proc. Natl. Acad. Sci. U.S.A. **109**, 9360–9365 (2012).

[20]G. D. John and T. M. Olsen, "Thermal hysteresis protein activity in bacteria, fungi and phylogenetically diverse plants," Cryobiology **30**, 322–328 (1993).

[21]W. Humphrey, A. Dalke, and K. Schulten, "VMD-visual molecular dynamics," Mol. Graphics **14**, 33–38 (1996).

[22]J. M. Siewert, H. J. Risselada, S. Yefimov, D. P. Tieleman, and H. D. Alex, "The MARTINI force field: Coarse grained model for biomolecular simulation," Phys. Chem. B **111**, 7812–7824 (2007).

[23]B. Hess, C. Kutzner, D. van der Spoel, and E. Lindahl, "GROMACS 4: Algorithms for highly efficient, load-balanced, and scalable molecular simulation," Chem. Theory Comput. **4**, 435–447 (2008).

[24] T. Darden, D. York, and J. Pedersen, "Particle mesh Ewald: An Nlog (N) method for Ewald sums in large systems," Chem. Phys. **98**, 10089–10092 (1993).

[25] H. J. C. Berendsen, J. P. M. Postma, W. F. V. Gunsteren, A. Dinola, and J. R. Haak, "Molecular dynamics with coupling to an external bath," Chem. Phys. **81**, 3684–3690 (1984).

[26] M. Parrinello, A. Rahman, "Polymorphic transitions in single crystals: A new molecular dynamics method," Appl. Phys. **52**, 7182–7190 (1981).

[27] R. W. Hockney, S. P. Goel, and J. Eastwood, "Quiet high resolution computer models of plasma," J. Comput. Phys. **14**, 148–158 (1974).

[28] L. M. Tamsin, J. M. Benjamin, V. B. Andrey, J. Anwar, and G. S. Christoph, "Structure of ice crystallized from supercooled water," Proc. Natl. Acad. Sci. U.S.A. **109**, 1041–1045 (2011).

[29] R. A. Nistor, T. E. Markland, and B. J. Berne, "Interface-limit growth of heterogeneously nucleated ice in supercooled water," Phys. Chem. B **118**, 752–760 (2014).